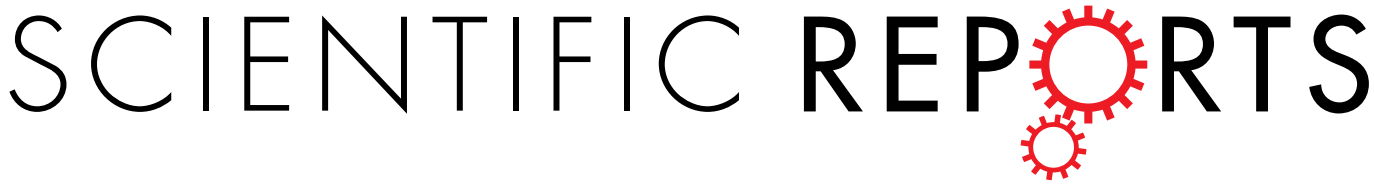

OPEN

Endothelial to mesenchymal transition contributes to arsenic-trioxide-induced cardiac fibrosis

Received: 05 April 2016
Accepted: 01 September 2016
Published: 27 September 2016

Yong Zhang[1,2,*], Xianxian Wu[1,*], Yang Li[3,*], Haiying Zhang[1], Zhange Li[1], Ying Zhang[1], Longyin Zhang[1], Jiaming Ju[1], Xin Liu[1], Xiaohui Chen[1], Peter V. Glybochko[4], Vladimir Nikolenko[4], Philipp Kopylov[5], Chaoqian Xu[1] & Baofeng Yang[1,6]

Emerging evidence has suggested the critical role of endothelial to mesenchymal transition (EndMT) in fibrotic diseases. The present study was designed to examine whether EndMT is involved in arsenic trioxide (As_2O_3)-induced cardiac fibrosis and to explore the underlying mechanisms. Cardiac dysfunction was observed in rats after exposure to As_2O_3 for 15 days using echocardiography, and the deposition of collagen was detected by Masson's trichrome staining and electron microscope. EndMT was indicated by the loss of endothelial cell markers (VE-cadherin and CD31) and the acquisition of mesenchymal cell markers (α-SMA and FSP1) determined by RT-PCR at the mRNA level and Western blot and immunofluorescence analysis at the protein level. In the *in-vitro* experiments, endothelial cells acquired a spindle-shaped morphology accompanying downregulation of the endothelial cell markers and upregulation of the mesenchymal cell markers when exposed to As_2O_3. As_2O_3 activated the AKT/GSK-3β/Snail signaling pathway, and blocking this pathway with PI3K inhibitor (LY294002) abolished EndMT in As_2O_3-treated endothelial cells. Our results highlight that As_2O_3 is an EndMT-promoting factor during cardiac fibrosis, suggesting that targeting EndMT is beneficial for preventing As_2O_3-induced cardiac toxicity.

The first application of arsenic trioxide (As_2O_3) to patients with acute promyelocytic leukemia (APL) can be traced back to 1970s when the scholars in the Harbin Medical University conducted a small-scale clinical trial on it[1,2]. Since then, As_2O_3 has been widely used not only in clinical but also in basic research, shedding new light on the treatment of many other cancers[3,4]. However, the clinical use of As_2O_3 is restricted due to its cardiotoxicity, including long QT syndrome (LQTS) and torsades de pointes which can lead to sudden cardiac death[5,6]. A recent study revealed that As_2O_3-induced fibrosis in cardiac fibroblasts (CFs) is involved in the development of LQTS[7]. Cardiac fibrosis, a common pathological feature of many heart diseases, is associated with the disruption of normal cardiac structures and functions resulting from the excessive production and deposition of ECM in the myocardium[8]. Cardiac fibrosis plays a decisive role in the generation and development of heart disease and is involved in numerous forms of cardiovascular diseases including myocardial infarction, hypertension, and heart failure[9–11].

Although accumulation of ECM proteins is an important characteristic in the fibrotic hearts, the mechanisms remain largely unknown. Myofibroblasts, characterized by α-smooth muscle actin (α-SMA) expression, are the primary determinant of cardiac fibrosis[12]. Myofibroblasts are mainly derived from resident fibroblasts, but recent studies revealed that they can also originate from transformation of vascular endothelial cells[13].

[1]Department of Pharmacology (the State-Province Key Laboratories of Biomedicine-Pharmaceutics of China, Key Laboratory of Cardiovascular Research, Ministry of Education), College of Pharmacy, Harbin Medical University, Harbin, 150081, China. [2]Institute of Metabolic Disease, Heilongjiang Academy of Medical Science, Harbin, 150086, China. [3]Center for Endemic Disease Control, Chinese Center for Disease Control and Prevention, Key Lab of Etiology and Epidemiology, Education Bureau of Heilongjiang Province & Ministry of Health (23618504), Harbin Medical University, Harbin, 150081, China. [4]The Research Center, Sechenov First Moscow State Medical University, Moscow, 119991, Russia. [5]Department of preventive and emergency cardiology, Sechenov First Moscow State Medical University, Moscow, 119991, Russia. [6]Department of Pharmacology and Therapeutics, Melbourne School of Biomedical Sciences, Faculty of Medicine, Dentistry and Health Sciences, The University of Melbourne, Melbourne, 3010, Australia. *These authors contributed equally to this work. Correspondence and requests for materials should be addressed to Yong Z. (email: hmuzhangyong@hotmail.com) or B.Y. (email: yangbf@ems.hrbmu.edu.cn)

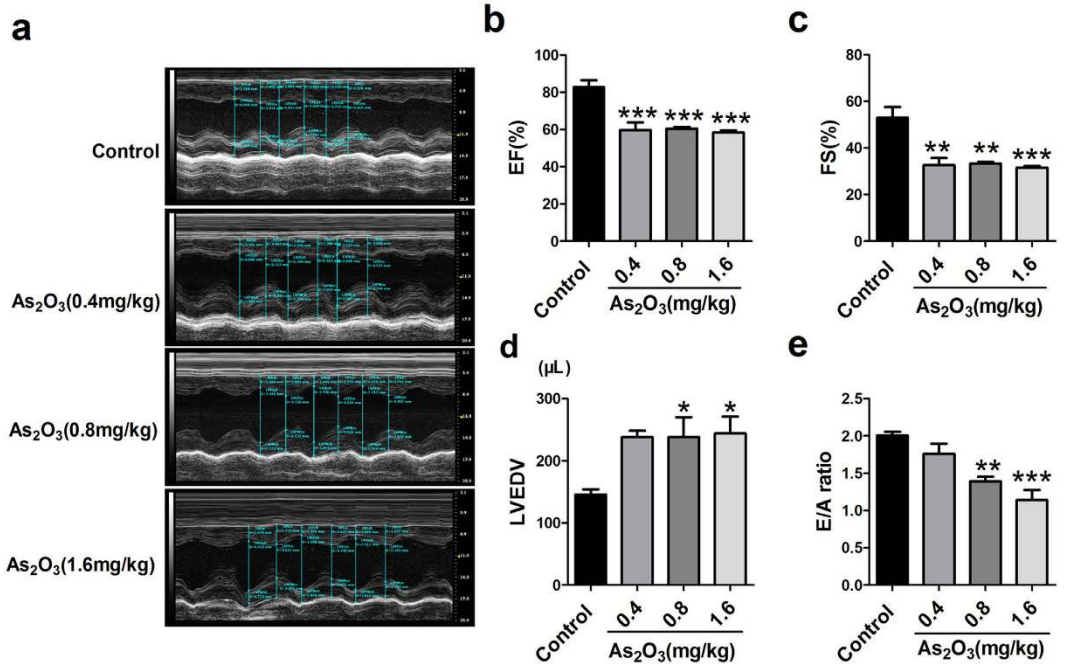

Figure 1. Effect of As_2O_3 on cardiac function determined by echocardiography. (**a**) Representative echocardiographic photos from M-mode. (**b**) Ejection fraction (EF) in each group. (**c**) Fraction shortening (FS) in each group. (**d**) Left ventricular end-diastolic volume (LVEDV) in each group. (**e**) Ratio of peak early diastolic ventricular filling velocity to peak atrial filling velocity (E/A). n = 4–5 rats in each group. *p < 0.05, **p < 0.01, ***p < 0.001 vs. Control.

The transformation of vascular endothelial cells into myofibroblasts is a process known as endothelial-to-mesenchymal transition (EndMT), which was first identified in the embryonic development of the heart[14]. As a special form of epithelial to mesenchymal transition (EMT), EndMT is also involved in the development of cardiac fibrosis and other fibrotic diseases[15–19]. During the process of EndMT, endothelial cells lose their original phenotypes and eventually transform into a mesenchymal or myofibroblastic phenotypes with adoption of the migratory properties and acquisition of mesenchymal cell markers such as α-SMA and fibrotic-specific protein 1(FSP1)[17]. Most notably, many studies have concentrated on this newly recognized type of cellular transformation, and they found that EndMT is an important source of activated fibroblasts and myofibroblasts that actively participate in stimulus-induced cardiac fibrosis especially perivascular fibrosis[20–23]. However, the relationship between As_2O_3, EndMT and perivascular fibrosis, and also the underlying mechanisms remain unexplored.

In the present study, we explored the potential role of As_2O_3 in triggering EndMT to form cardiac fibrosis, and investigated the signaling pathway leading to EndMT in human aortic endothelial cells (HAECs).

Results

As_2O_3 impairs cardiac function in Wistar rats. The adverse effects of As_2O_3 on the heart have been reported in both clinical practice and basic research[24,25]. After two weeks of As_2O_3 administration, we performed echocardiographic measurements to evaluate the effect of As_2O_3 on cardiac function. The corresponding echocardiographic images in the control group and As_2O_3-treated groups (0.4 mg/kg, 0.8 mg/kg, 1.6 mg/kg) are shown in Fig. 1a. The ejection fraction (EF%) declined significantly from 82.83 ± 3.72% for control to 59.68 ± 4.21%, 60.57 ± 0.90% and 58.44 ± 1.06% for varying dosages of As_2O_3, respectively (Fig. 1b). Moreover, the fractional shortening (FS%) decreased dramatically from 53.03 ± 4.61% to 32.73 ± 2.96%, 33.33 ± 0.71% and 31.55 ± 0.73%, respectively (Fig. 1c). Additionally, we detected left ventricular end-diastolic volume (LVEDV) and ratio of peak early diastolic ventricular filling velocity to peak atrial filling velocity (E/A), which can be used as indicative markers of diastolic dysfunction. The results in Fig. 1d–e showed that LVEDV was elevated, while the E/A ratio was declined after exposure to As_2O_3. But this effect was only statistically significant at the dosages of 1.6 mg/kg and 0.8 mg/kg. The detailed data for end-systolic and end-diastolic volumes and other additional parameters were also provided (Supplementary Table 2). All of these data indicated that cardiac dysfunction appeared when the rats received As_2O_3 treatment.

As_2O_3 induces cardiac fibrosis . Excessive production and deposition of extracellular matrix (ECM) proteins are the primary characteristic of cardiac fibrosis. To verify whether As_2O_3 could induce cardiac fibrosis, Masson's trichrome staining and transmission electron microscopy were performed. Collagen production and deposition increased markedly in the As_2O_3-treated groups compared with the control group in both perivascular region and intramyocardial region (Fig. 2a). Meanwhile, the transmission electron microscopy images demonstrated that exposure to As_2O_3 (1.6mg/kg) significantly increased ECM deposition compared with the control

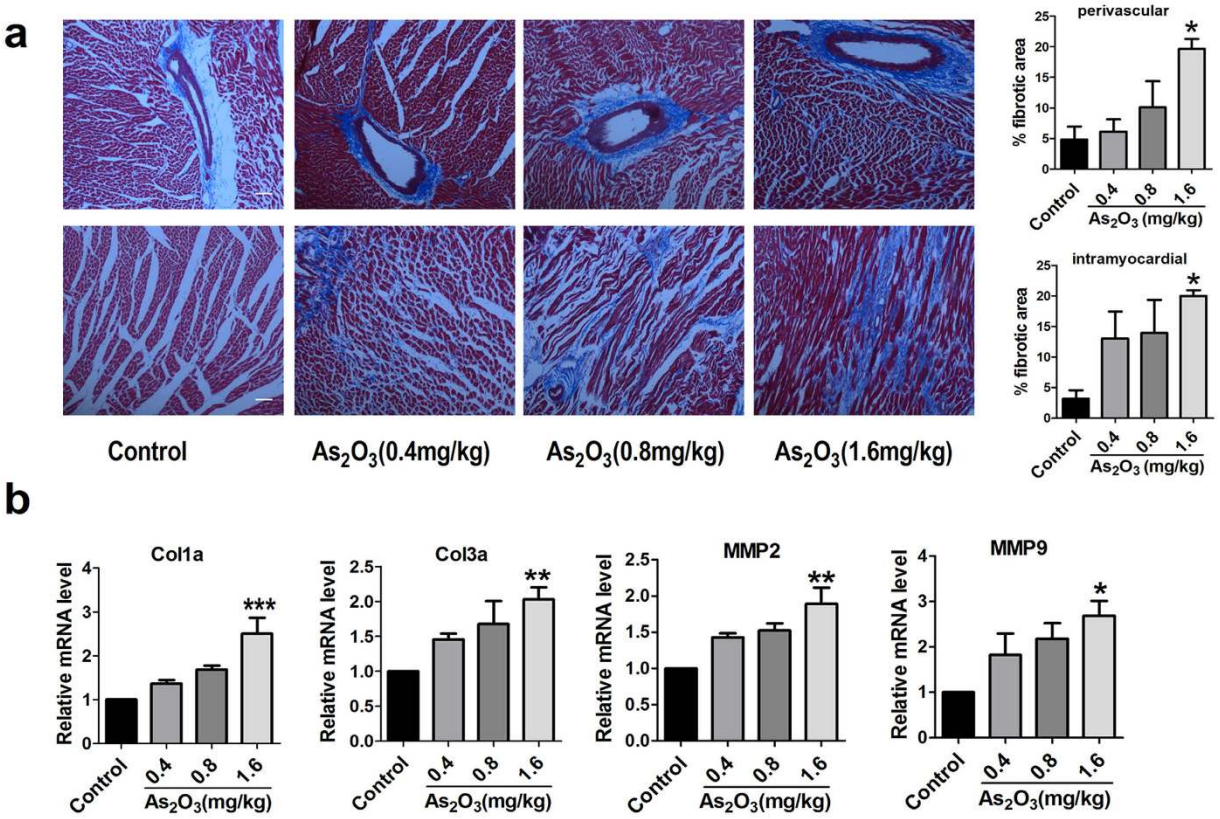

Figure 2. Collagen production and fibrotic gene expression in As_2O_3-treated animal models. (**a**) Masson trichrome staining for collagen deposition in cardiac cross-sectional parts. Collagen is indicated as blue areas, scale bar = 200 μm. (**b**) mRNA expression level of the fibrosis-related genes Col1a, Col3a, mmp2, mmp9. *p < 0.05, **p < 0.01, ***p < 0.001 vs. Control. Graph bars represent mean ± SEM, n = 3–5.

group (Supplementary Figure 1). Additionally, qRT-PCR results revealed that the expression of pro-fibrotic genes including Col1a, Col3a, mmp2 and mmp9 was upregulated in the As_2O_3-treated groups (Fig. 2b). However, it should be noted that significant effects of As_2O_3 on cardiac fibrosis were seen only at the high-dose group, even though the same trend of changes was also observed with lower dosages.

EndMT is present in As_2O_3-induced cardiac fibrosis. Accumulating evidence suggests that EndMT is an important contributor to cardiac fibrosis[15]. Therefore, we investigated whether As_2O_3 induced cardiac fibrosis was mediated by EndMT. As shown in Fig. 3a,b, the downregulation of endothelial–specific markers (VE-cadherin and CD31) and upregulation of mesenchymal markers (α-SMA and FSP1) were observed in hearts of As_2O_3 treated rats. However, these changes were only statistically significant at the high-dose group, but not at the two lower dose groups, especially for the expression of mesenchymal markers. Meanwhile, we obtained similar results using qRT-PCR analysis (Fig. 3c). Moreover, the expression of typical transcriptional factors (Snail, Twist, Slug) for EndMT was also markedly increased at the high-dose group (Supplementary Figure 2). We next performed double immunofluorescence staining of CD31 (green) and α-SMA (red) for EndMT and observed the co-localization of CD31 and α-SMA in myocardial sections of rats with the high-dose As_2O_3 (Fig. 3d). All of these results suggest that EndMT might be involved in As_2O_3-induced cardiac fibrosis.

As_2O_3 treatment triggers EndMT in HAECs. To further elucidate the relationship between As_2O_3 and EndMT, we used HAECs for our subsequent *in vitro* experiments. After treatment with varying concentrations of As_2O_3 for 24 h, the endothelial cells underwent a morphological transformation to fibroblast-like spindle-shaped phenotype (Fig. 4a). However, we should note that the morphological change of endothelial cells at the concentration of 2 μmol/l was not as obvious as that at 4 μmol/l and 8 μmol/l. When we prolong the treatment time to 48 h and 72 h, this change became more remarkable (Fig. 4b). Besides, As_2O_3 reduced the expression of endothelial cell markers (VE-cadherin and CD31) and augmented the expression of mesenchymal markers (α-SMA and FSP1) in a concentration-dependent manner as indicated by western blotting results (Fig. 4c). Similar results were obtained with qRT-PCR analysis (Fig. 4d). Additionally, we detected two other mesenchymal markers fibronectin (FN) and vimentin and found that the expression of FN and vimentin had the same trend as the expression of α-SMA and FSP1 (Fig. 4d). Meanwhile, the mRNA levels of fibrotic-related genes, including Col1a, Col3a, mmp2 and mmp9, were markedly increased (Fig. 4e). The results from double immunofluorescence staining further confirmed that endothelial cells with As_2O_3 treatment underwent EndMT with a decrease for the membrane

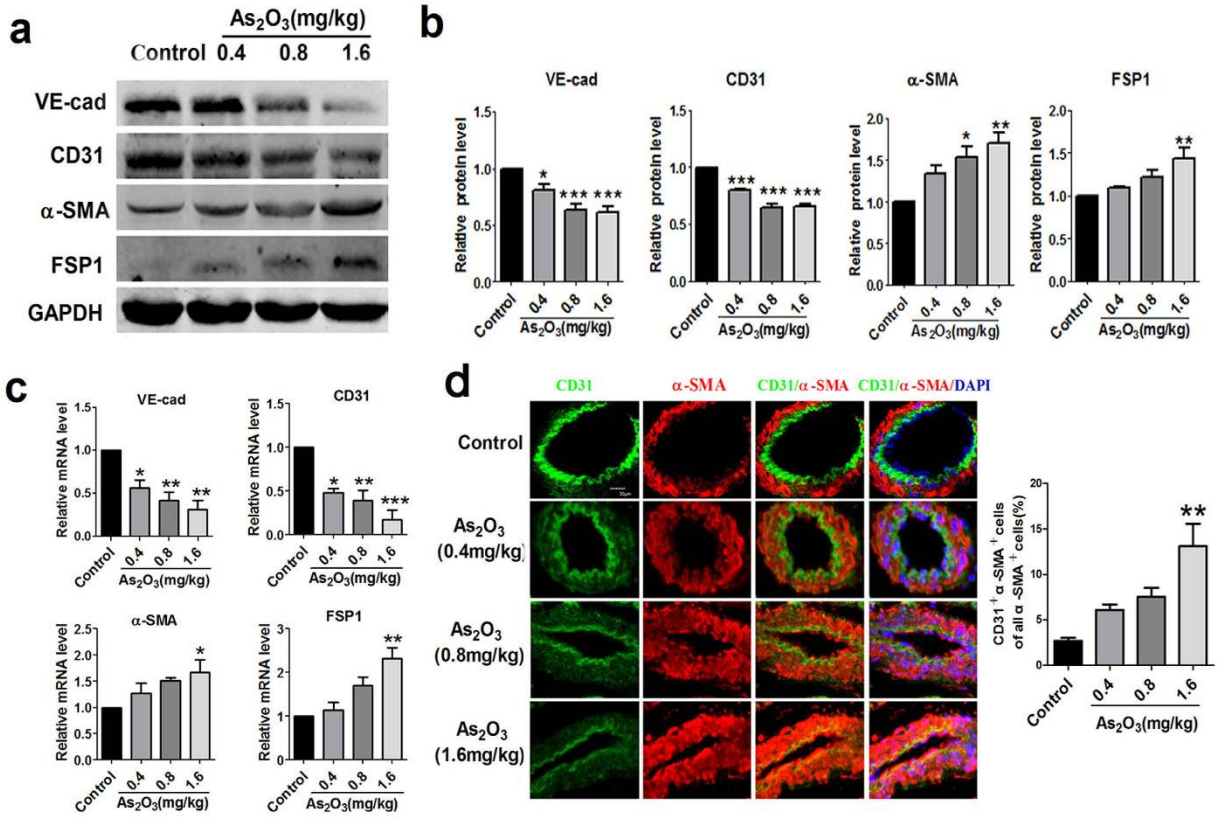

Figure 3. EndMT in As_2O_3-induced cardiac fibrosis. (**a**) Representative protein bands of endothelial markers VE-cadherin (VE-cad) and CD31 and mesenchymal markers α-smooth muscle actin (α-SMA) and fibroblast-specific protein-1 (FSP1) in cardiac tissues by western blotting. (**b**) Analysis of western blotting results normalized to glyceraldehyde phosphate dehydrogenase (GAPDH). (**c**) Quantitative real-time PCR experiments for relative mRNA levels of VE-cad, CD31, α-SMA, FSP1. No significant difference was observed between the different dosages groups. *$p < 0.05$, **$p < 0.01$, ***$p < 0.001$ vs. Control. Data are expressed as mean ± SEM, n = 3–5. (**d**) Double immunofluorescence labeling of CD31 (green) and α-SMA (red) in As_2O_3 treated hearts, nuclei are stained with DAPI (blue). Yellow indicates co-localization of CD31 with α-SMA expression in vessels. Scale bar = 30 μm. **$p < 0.01$ vs. Control, n = 3.

staining of CD31 and increase for the cytoplasm staining of α-SMA (Fig. 4f). Taken together, we have demonstrated that As_2O_3 could elicit EndMT in HAECs.

The AKT/GSK-3β/Snail pathway is activated in As_2O_3-mediated EndMT. Multiple signaling pathways are involved in the process of EndMT, such as the TGF-β pathway, Notch pathway, and PI3K/AKT pathway[26–29]. The AKT/GSK-3β/Snail pathway has been proposed to play an important role in inducing EMT[30,31]. Because EndMT is a special form of EMT, here we hypothesized that As_2O_3 may induce EndMT via the AKT/GSK-3β/Snail pathway. As expected, upon treatment with a high concentration of As_2O_3 (8 μmol/l) for 24 h, phosphorylation of AKT and GSK-3β was dramatically increased and Snail expression was significantly enhanced in HAECs. The total protein and mRNA levels of AKT and GSK-3β were unaffected by As_2O_3 at concentrations of 2, 4 and 8 μmol/l (Fig. 5a,b). To further demonstrate the phenomenon of AKT/GSK-3β/Snail signaling activation *in vivo*, we double-stained CD31/p-AKT, CD31/p-GSK-3β and CD31/Snail in heart tissues. The results in Supplementary Figure 3 showed that the expression of p-AKT, p-GSK-3β and Snail were at a higher level in endothelial cells of myocardial sections from As_2O_3-treated rats, which suggested that the AKT/GSK-3β/Snail signaling pathway is also activated *in vivo*.

Blocking As_2O_3-induced phosphorylation of AKT inhibits EndMT in HAECs. To clarify the role of the AKT/ GSK-3β/Snail pathway in As_2O_3-induced EndMT, LY294002 (an inhibitor of PI3K/AKT) was used to treat HAECs prior to As_2O_3 treatment. As shown in Fig. 6a, the expression levels of phosphorylated AKT, phosphorylated GSK-3β and Snail were markedly increased after As_2O_3 treatment, whereas these effects were prevented upon pre-treatment with LY294002 in combination with As_2O_3 in HAECs. But the protein and mRNA level of AKT and GSK-3β were not affected by LY294002 (Fig. 6a,b). Notably, we found that pre-treatment with LY294002 abrogated the morphological conversion of HAECs induced by As_2O_3 (Fig. 6c). While LY294002 applied alone did not exert much influence on cells phenotype in comparison to control group.

We also detected EndMT-associated markers in the condition of AKT pathway inhibition. Western blotting analysis showed that LY294002 effectively prevented the downregulation of endothelial markers and upregulation

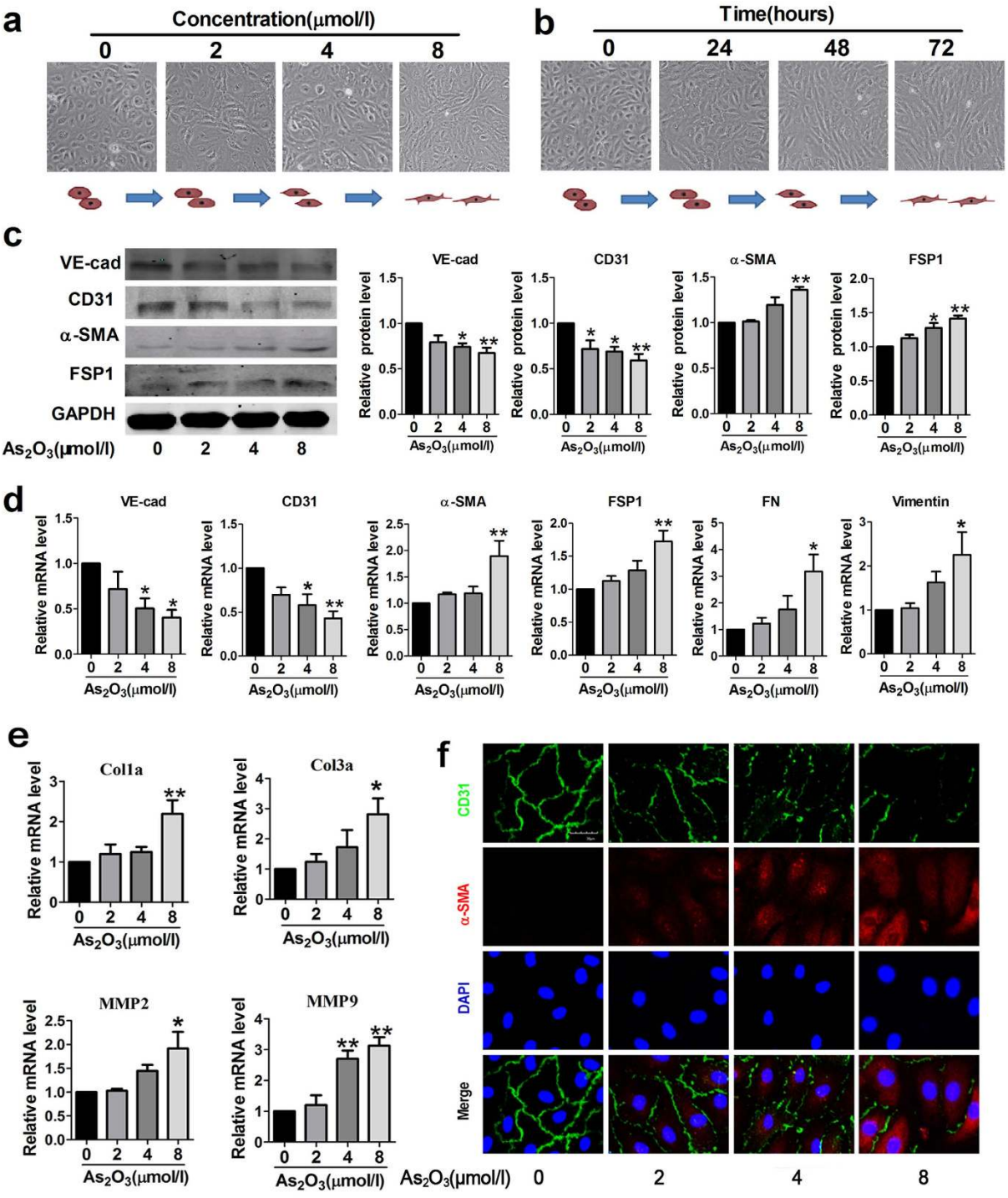

Figure 4. As_2O_3 triggers EndMT in human aortic endothelial cells (HAECs). (**a**) Morphological changes of endothelial cells exposed to different concentrations of As_2O_3. (**b**) Morphological changes of endothelial cells treated with As_2O_3 (2 μmol/l) for 0, 24, 48 or 72 hours. (**c**) Western blotting results for relative protein levels of VE-cad, CD31, α-SMA and FSP1 in As_2O_3-treated HAECs. GAPDH was used as an internal control. (**d**) Relative expression levels of endothelial markers (VE-cad, CD31) and mesenchymal markers (α-SMA, FSP1, FN and Vimentin) were compared by qRT-PCR between control groups and As_2O_3-treated groups. FN, fibronectin. (**e**) Relative mRNA levels of fibrosis-related genes Col1a, Col3a, mmp2 and mmp9. (**f**) Representative confocal microscopy images showing staining of endothelial marker CD31 and mesenchymal marker α-SMA in As_2O_3-treated HAECs. Scale bar = 30 μm. $^*p < 0.05$, $^{**}p < 0.01$ vs. untreated condition (0 μmol/l As_2O_3). No significant difference was observed between the different concentrations groups. Data are represented as mean ± SEM, n = 3–5.

of mesenchymal markers by As_2O_3 (Fig. 7a). Consistently, the qRT-PCR results revealed that the As_2O_3-induced reduction of endothelial markers and augmentation of mesenchymal markers and fibrosis-related gene expression

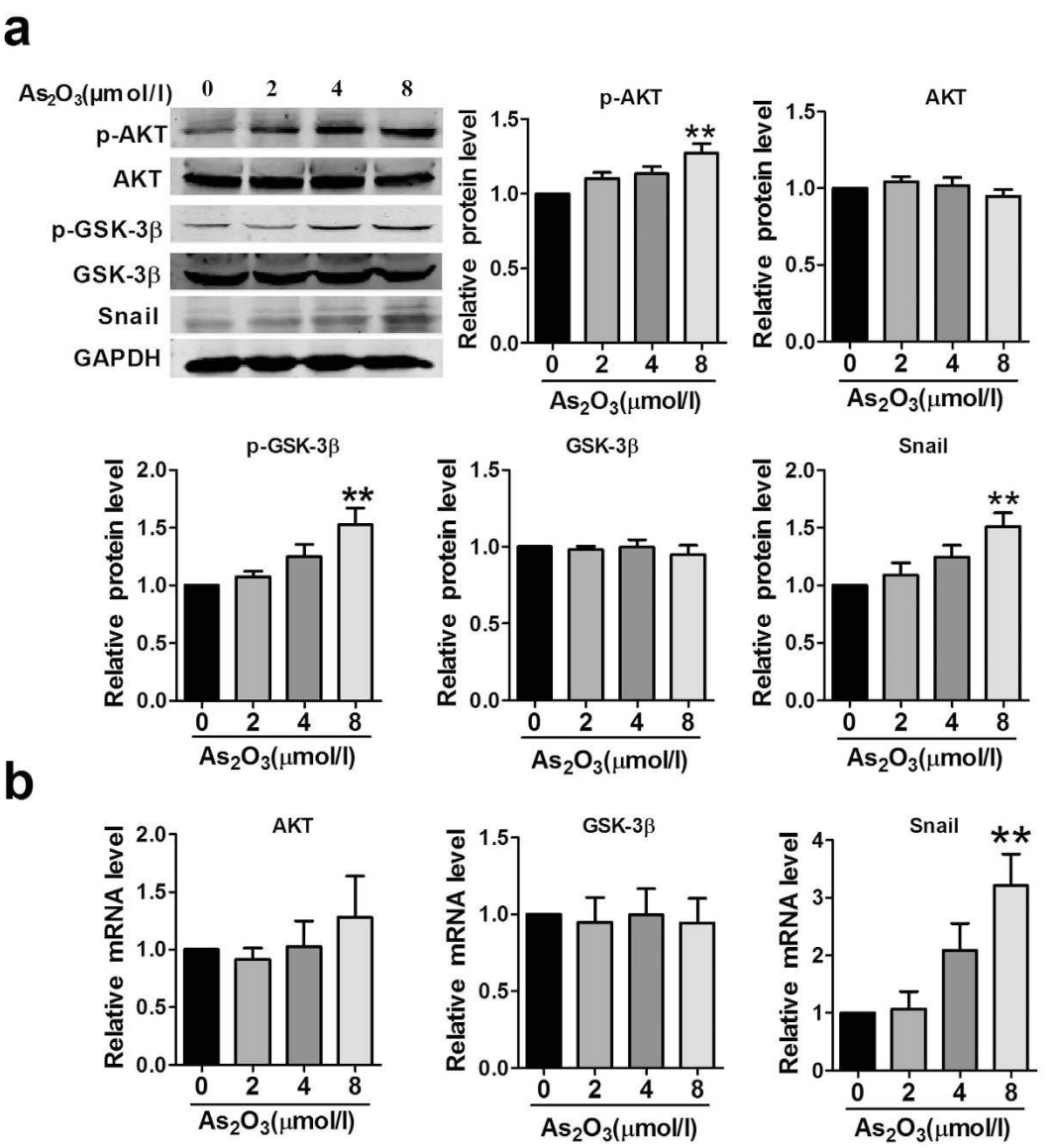

Figure 5. As_2O_3 activates the AKT/GSK-3β/Snail pathway. (**a**) HAECs were treated with or without As_2O_3, and the expression of Snail and the activation of AKT and GSK-3β were determined by western blotting. (**b**) Relative mRNA expression level of AKT, GSK-3β and Snail in different groups. $^{**}p < 0.01$ vs. untreated condition (0 μmol/l As_2O_3). Data are expressed as mean ± SEM, n = 3–5.

were attenuated by pre-treatment with LY294002 (Fig. 7b,c). Moreover, the immunostaining assay confirmed the inhibitory effects of the PI3K inhibitor (LY294002) on EndMT (Fig. 7d).

Discussion

In the present study, we made an effort to understand the potential role of EndMT in As_2O_3-induced cardiac fibrosis. First, *in vivo* study showed that EndMT was present in the progression of cardiac fibrosis and cardiac dysfunction. Second, *in vitro* study confirmed that As_2O_3 could result in EndMT in HAECs, and this process was partly mediated by the AKT/GSK-3β/Snail pathway. The proposed mechanism is illustrated in Fig. 8.

Cardiac fibrosis, as an adaptive response or repair mechanism, can be defined as excessive deposition of ECM components in the cardiac interstitium. Studies have found that cardiac fibrosis leads not only to heart failure but also to fatal arrhythmia[32,33], which can be attributed to the reduction of cardiac contractility and compliance. Therefore, we have a reason to believe that myocardial fibrosis is responsible for the induction of cardiac toxicity in APL patients receiving As_2O_3 therapy or in conditions of arsenic exposure. Clinically, As_2O_3 is administrated intravenously at dosages of 10 mg/d for adults and 0.16 mg/kg for children[34,35]. Pharmacokinetic studies showed that the mean peak level of As_2O_3 in plasma is 6.85 μmol/l[34]. The dosages of As_2O_3 tested in our *in vivo* studies (0.4, 0.8 and 1.6 mg/kg) fall right within this clinical range and are also in accordance with the published studies relevant to the cardiotoxicity of As_2O_3[7,36]. Moreover, the concentration range of As_2O_3 (2~8 μmol/l) used in our *in vitro* study encompasses the clinically relevant concentrations.

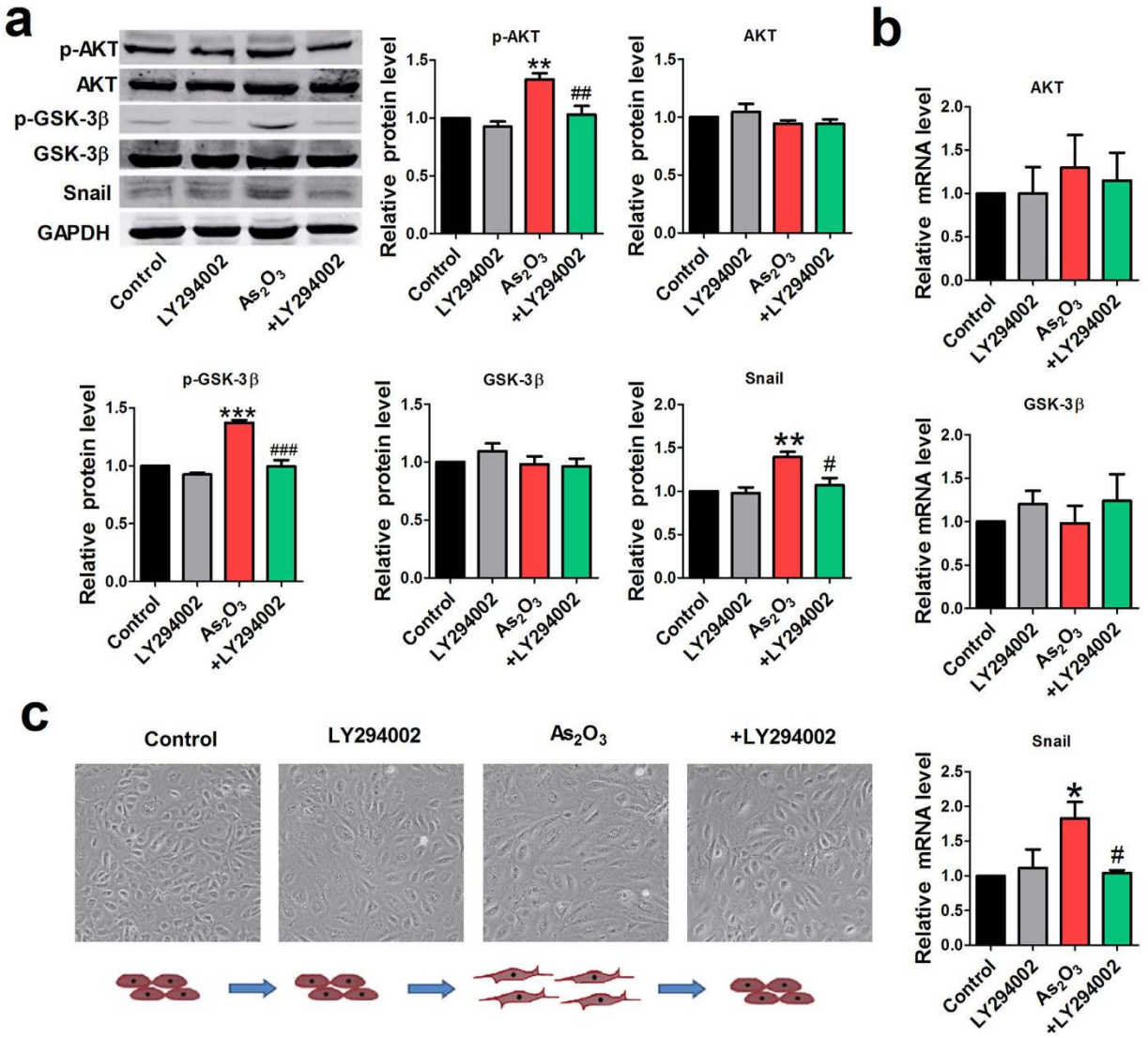

Figure 6. Effects of the PI3K inhibitor LY294002 on the AKT/GSK-3β/Snail pathway and EndMT phenotypes in HAECs. (**a**) Before treatment with As_2O_3 (8 μmol/l), HAECs were pretreated with LY294002 for 2 h. The activation of AKT and GSK-3β and the expression of snail were analyzed by western blotting. +LY294002 indicates the co-application of LY294002 and As_2O_3 (8 μmol/l). (**b**) Relative mRNA level of AKT, GSK-3β and snail in different groups. $^{*}p < 0.05$, $^{**}p < 0.01$, $^{***}p < 0.001$ vs. Control. $^{\#}p < 0.05$, $^{\#\#}p < 0.01$, $^{\#\#\#}p < 0.001$ vs. As_2O_3. Data are shown as mean ± SEM, n = 3–5. (**c**) Effects of LY294002 on the morphologic phenotype of HAECs.

Traditionally, the activation and proliferation of resident fibroblasts are considered a key source of myofibroblasts in cardiac fibrosis. Many anti-fibrotic agents are focused on inhibiting cardiac fibroblast proliferation and collagen production[37,38]. Recently, EndMT was found to be as an alternative origin of myofibroblasts and to play an increasingly important role in the development of cardiac fibrosis. A study by Zeisberg E.M. *et al.* first demonstrated the contribution of EndMT to the total pool of cardiac fibroblasts. They used fate mapping method to identify the origin of cardiac fibroblasts and found that endothelial cells are responsible for the emergence of fibroblasts[15]. Another study by Widyantoro *et al.* showed that endothelial cell-derived endothelin-1 (ET-1) could stimulate the EndMT process and promote diabetes mellitus–induced cardiac fibrosis[23]. Moreover, Rining Tang and colleagues revealed that high glucose-induced EndMT is mediated by angiotensin II and this process could be inhibited by Irbesartan[39]. Furthermore, Ignacio Montorfano *et al.* found that oxidative stress could induce the conversion of endothelial cells into myofibroblasts through the TGF-β dependent pathway[40]. All of these findings underline the prevalence of EndMT in cardiac fibrosis.

EndMT is a process of cellular transdifferentiation with similarities to epithelial-to-mesenchymal transition (EMT) in which endothelial cells lose their cell-cell junctions, change their morphology into a mesenchymal or myofibroblastic phenotype, express mesenchymal cell markers and gain migratory or contractile properties. Here we performed confocal microscopy analysis to assess the co-localization of CD31 (endothelial marker) and α-SMA (mesenchymal marker) in As_2O_3-treated heart tissues. Co-expression of the endothelial marker CD31

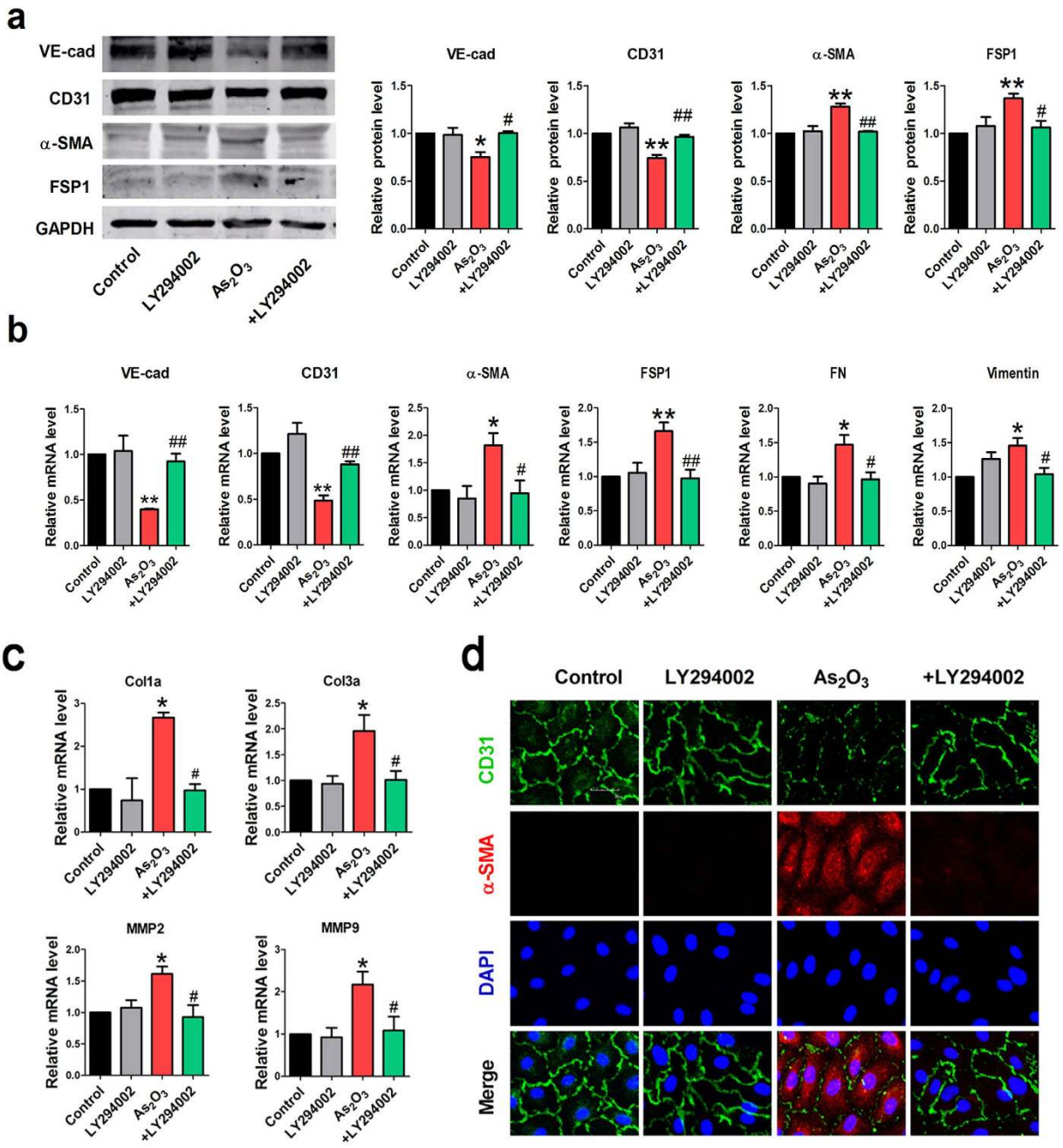

Figure 7. PI3K inhibitor LY294002 represses As_2O_3-induced EndMT in HAECs. (**a**) Western blotting results for relative protein levels of VE-cad, CD31, α-SMA and FSP1 in different groups. +LY294002 indicates the co-application of LY294002 and As_2O_3 (8 μmol/l). (**b**) Relative mRNA expression levels of VE-cad, CD31, α-SMA, FSP1, FN and Vimentin in each group by qRT-PCR analysis. (**c**) Effects of LY294002 on the mRNA expression of fibrosis-related genes Col1a, Col3a, mmp2, mmp9. $^{*}p < 0.05$, $^{**}p < 0.01$ vs. Control. $^{\#}p < 0.05$, $^{\#\#}p < 0.01$ vs. As_2O_3. Data are shown as mean ± SEM, n = 3–5. (**d**) Immunofluorescence analysis for the expression levels of CD31 and α-SMA in Control, LY294002, As_2O_3 and As_2O_3 + LY294002 groups. Scale bar = 30 μm.

with mesenchymal marker α-SMA or FSP1 indicates the intermediate stage of EndMT[41,42]. Our observations suggested the participation of EndMT in As_2O_3-induced cardiac fibrosis. Meanwhile, we found that As_2O_3 induced endothelial cells undergo morphological changes in a concentration-dependent manner, but the changes were mostly visible at a concentration of 8 μmol/l. Moreover, the expression of VE-cadherin and CD31 was decreased and the expression of α-SMA and FSP1 was increased, which indicates the occurrence of EndMT. Nevertheless, the morphological change of the HAECs was not obvious at an As_2O_3 concentration of 2 μmol/l. However, when we prolonged the treatment time to 48 h and 72 h, the phenotypic change of the endothelial cells became apparent.

The AKT/ GSK-3β/Snail pathway is an important pathway involved in the process of EMT[30,43]. EndMT shares some similarities with EMT including the underlying mechanisms. However, it remains elusive whether this

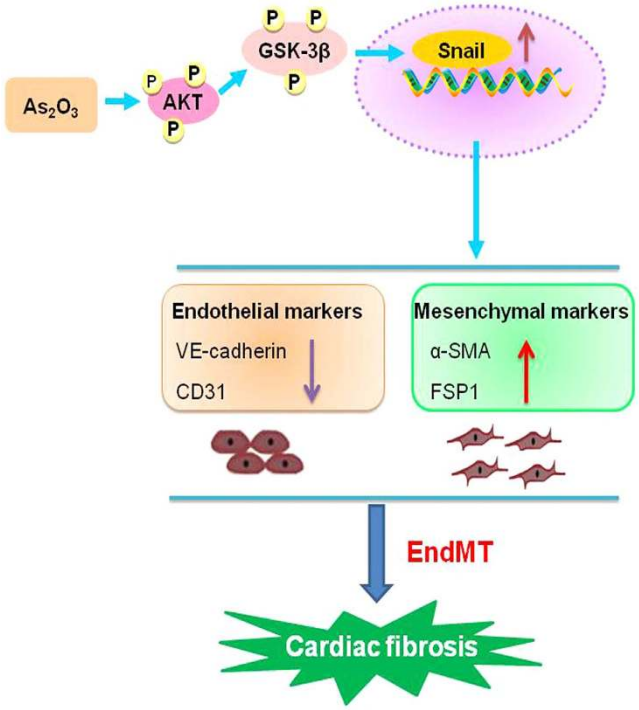

Figure 8. A schematic diagram revealing the underlying mechanisms of As_2O_3 induced EndMT and cardiac fibrosis.

pathway participates in the process of EndMT. As a transcription factor that suppresses cell adhesion, snail has been widely studied in EMT and EndMT. GSK-3β kinase phosphorylation was once thought to be a crucial event during EndMT[44]. Snail can induce EndMT when the activity of GSK-3β is inhibited by PI3K signaling or with LiCl[45]. Our study demonstrated that As_2O_3 treatment (8 μmol/l) activated the AKT/GSK-3β/snail pathway in HAECs, and this phenomenon could be prevented by the PI3K inhibitor LY294002. What is more, LY294002 could abolish the process of EndMT induced by As_2O_3, which suggests that the AKT/GSK-3β/Snail signaling pathway is also involved in promoting EndMT. Our study did not exclude critical roles of other transcriptional factors and signaling pathways in the process of As_2O_3-induced EndMT. And also, it must be noted that the effect of PI3K/AKT inhibitor was detected only in cultured endothelial cells, the results may not be directly applicable to *in vivo* conditions. The *in vivo* role of the AKT/GSK-3β/Snail signaling pathway remains to be explored in the future.

It has been reported that As_2O_3 is capable of producing reactive oxide species (ROS)[46], which might be responsible for the activation of PI3K/AKT. Our results in Supplementary Figure 4 demonstrated this point. But much more detailed studies are needed to further demonstrate the role of ROS in the process of EndMT.

Overall, our present study unraveled that As_2O_3 can induce EndMT in HAECs via the AKT/GSK-3β/Snail pathway and that EndMT might be involved in As_2O_3-induced cardiac fibrosis. The results of this study suggest that blocking EndMT may provide a viable therapeutic strategy against As_2O_3-induced cardiac fibrosis and cardiac dysfunction.

Methods

Animal experiments and ethics statements. Healthy male Wistar rats (200–250 g) were obtained from the Experimental Animal Center of the 2nd Affiliated Hospital of Harbin Medical University (Harbin, China). The rats were housed in a standard animal room with constant temperature (23 ± 1 °C) and humidity (55 ± 5%) and subjected to a 12-h light-dark cycle. The rats were randomly divided into four groups: Control, As_2O_3 (0.4 mg/kg, 0.8 mg/kg, 1.6 mg/kg). As_2O_3 was provided by Harbin YI-DA Pharmaceutical Limited Company and administered intravenously every other day for two weeks. The dosage used in this study was based on previous studies[7,47]. The animal experiments were performed under the guidelines from Directive 2010/63/EU of the European Parliament on the protection of animals used for scientific purposes. All the procedures were approved by the Institutional Animal Care and Use Committee of the Harbin Medical University, China [SYXK 2011-033 (2011.12.13 –2016.12.12)].

Echocardiography. After two weeks of As_2O_3 administration, all of the rats were anesthetized with sodium pentobarbital (40 mg/kg, i.p.). The absence of withdrawal reflex to tail pinch was used for monitoring of the adequacy of anaesthesia. After that the rats were prepared for detection of cardiac function with an ultrasound machine (Vivid 7, GE Medical System, USA) as previously described[48]. The following parameters were obtained: interventricular septum (IVS), left ventricular internal dimension (LVID), left ventricular posterior wall (LVPW),

ejection fraction (EF), fractional shortening (FS), left ventricular end-diastolic volume (LVEDV), left ventricular mass (LV mass), Left Ventricular end-systolic Volume (LVESV) and the ratio of peak early diastolic ventricular filling velocity to peak atrial filling velocity (E/A).

Evaluation of collagen deposition. Masson's trichrome staining and transmission electron microscopy were applied to observe collagen deposition as described previously[49]. Biriefly, following echocardiographic recordings, rats were euthanized by cervical dislocation method for heart tissues, which were cut into different parts. One part was fixed in 4% paraformaldehyde and then embedded in paraffin and sliced cross-sectionally into 5 μm sections for Masson's trichrome. Masson's trichrome staining was examined by light microscopy and the images were analyzed with Image Pro Plus software to quantify collagen percentage. For transmission electron microscopy, specimens were prepared and processed by routine methods as previously described[7].

Cell culture. Primary HAECs were purchased from Sciencell (No. 6100) and maintained in collagen-coated flasks with endothelial basal medium (ECM, Sciencell, No. 1001). The cells were cultured at 37 °C with 5% CO_2, and the medium was changed every 48 hours. When the culture reached 70% confluence, the cells were treated with various concentrations of As_2O_3 (2, 4 and 8 μM) for 24 h. The PI3K inhibitor LY294002 was obtained from Cayman chemical company (Ann Arbor, Michigan, USA), which was used to inhibit the phosphorylation of AKT in HAECs at a concentration of 20 μM.

RNA extraction and real-time quantitative RT-PCR (qRT-PCR). Total RNA was extracted from cardiac tissues and HAECs using TRIZOL reagent (Invitrogen, USA) as previously described[50,51], and then it was reverse transcribed into cDNA with a High-Capacity cDNA Reverse Transcription Kit (Applied Biosystems, Foster City, CA, USA) according to the manufacturer's instructions. Real-time PCR was performed to determine mRNA expression levels with an ABI 7500 fast Real Time PCR system (Applied Biosystems, USA). GAPDH was used as an internal control. The sequences of the primers are presented in Supplementary Table 1.

Protein extraction and western blot analysis. Protein samples were extracted from tissues and cells with the same procedures described previously[52,53]. Briefly, heart tissues and HAECs were lysed in RIPA buffer and then centrifuged at 4 °C 13500 rpm for 15 minutes. The supernatant was collected, and protein concentrations were determined by bicinchoninic acid (BCA) protein assay (Beyotime, Shanghai, China). Protein extracts were separated by SDS–PAGE and transferred onto a nitrocellulose membrane. The membranes were blocked and incubated with the following primary antibodies: anti-VE-cadherin antibody, anti-CD31 antibody, anti-α-SMA antibody, anti-FSP1 antibody, anti-Snail antibody (Abcam, Cambridge, MA, USA), anti-p-AKT antibody, anti-AKT antibody, anti-p-GSK-3β antibody, anti-GSK-3β antibody (Wanleibio. Shenyang, China), and anti-GAPDH antibody (Kangcheng, Shanghai, China); GAPDH was used as a loading control. After incubation at 4 °C overnight, the membrane was washed three times with PBST, incubated with fluorescence-conjugated goat anti-rabbit IgG and goat anti-mouse IgG for one hour at room temperature (1:10000, Invitrogen) and scanned by Odyssey Imaging System (LI-COR, Inc., Lincoln, NE, USA).

Immunofluorescence. Immunofluorescence staining was performed to detect the expression of CD31 and α-SMA in HAECs. Briefly, the cells were cultured on coverslips and received the desired treatment. At the end of the treatment, the cells were washed with PBS and processed in the same way as previously described[38]. For *in vivo* study, frozen heart tissues were cut into 5 μm thick sections to detect the phenomenon of EndMT. The secondary antibodies conjugated with Alexa Fluor 594 and Alexa Fluor-488 (Invitrogen, Carlsbad, CA, USA) were used in this experiment. Double positive labeling of CD31 and α-SMA was regarded as cell transformation. The immunofluorescence-labeled cells and tissues were examined and analyzed by laser scanning confocal microscopy (FV300, Olympus, Japan).

Statistical analysis. Results are expressed as mean ± SEM and were analyzed by one-way analysis of variance (ANOVA) with GraphPad Prism 5.0 software. $P < 0.05$ was considered statistically significant.

References

1. Zhang, T., Zhang, P., Wang, S. & Han, T. Preliminary clinical observations of 6 cases of leukemia treated by "Ailin solution". *Med Pharm Heilongjiang*. **3,** 66–67 (1973).
2. Cyranoski, D. Arsenic patent keeps drug for rare cancer out of reach of many. *Nat Med*. **13,** 1005 (2007).
3. Gazitt, Y. & Akay, C. Arsenic trioxide: an anti cancer missile with multiple warheads. *Hematology*. **10,** 205–213 (2005).
4. Zhai, B. *et al.* Arsenic trioxide potentiates the anti-cancer activities of sorafenib against hepatocellular carcinoma by inhibiting Akt activation. *Tumour Biol*. **36,** 2323–2334 (2015).
5. Singer, J. W. Cardiac toxicity of arsenic trioxide. *Blood*. **98,** 1633; author reply 1633–1634 (2001).
6. Naito, K. *et al.* Two cases of acute promyelocytic leukemia complicated by torsade de pointes during arsenic trioxide therapy. *Int. J. Hematol.* **83,** 318–323 (2006).
7. Chu, W. *et al.* Arsenic-induced interstitial myocardial fibrosis reveals a new insight into drug-induced long QT syndrome. *Cardiovasc. Res.* **96,** 90–98 (2012).
8. Weber, K. T. Fibrosis and hypertensive heart disease. *Curr. Opin. Cardiol.* **15,** 264–272 (2000).
9. Xu, L. *et al.* MMI-0100 inhibits cardiac fibrosis in myocardial infarction by direct actions on cardiomyocytes and fibroblasts via MK2 inhibition. *J Mol Cell Cardiol*. **77,** 86–101 (2014).
10. Fan, D., Takawale, A., Lee, J. & Kassiri, Z. Cardiac fibroblasts, fibrosis and extracellular matrix remodeling in heart disease. *Fibrogenesis Tissue Repair*. **5,** 15 (2012).
11. Piek, A., de Boer, R. A. & Sillje, H. H. The fibrosis-cell death axis in heart failure. *Heart Fail Rev*. **21,** 199–211 (2016).
12. Nagpal, V. *et al.* MiR-125b Is Critical for Fibroblast-to-Myofibroblast Transition and Cardiac Fibrosis. *Circulation*. **133,** 291–301 (2016).

13. Feng, B. *et al.* miR-200b Mediates Endothelial-to-Mesenchymal Transition in Diabetic Cardiomyopathy. *Diabetes*. **65,** 768–779 (2016).
14. Eisenberg, L. M. & Markwald, R. R. Molecular regulation of atrioventricular valvuloseptal morphogenesis. *Circ. Res.* **77,** 1–6 (1995).
15. Zeisberg, E. M. *et al.* Endothelial-to-mesenchymal transition contributes to cardiac fibrosis. *Nat Med*. **13,** 952–961 (2007).
16. Kovacic, J. C., Mercader, N., Torres, M., Boehm, M. & Fuster, V. Epithelial-to-mesenchymal and endothelial-to-mesenchymal transition: from cardiovascular development to disease. *Circulation*. **125,** 1795–1808 (2012).
17. Piera-Velazquez, S. & Jimenez, S. A. Molecular mechanisms of endothelial to mesenchymal cell transition (EndoMT) in experimentally induced fibrotic diseases. *Fibrogenesis Tissue Repair*. **5,** S7 (2012).
18. He, J., Xu, Y., Koya, D. & Kanasaki, K. Role of the endothelial-to-mesenchymal transition in renal fibrosis of chronic kidney disease. *Clin Exp Nephrol*. **17,** 488–497 (2013).
19. Ranchoux, B. *et al.* Endothelial-to-mesenchymal transition in pulmonary hypertension. *Circulation*. **131,** 1006–1018 (2015).
20. Murdoch, C. E. *et al.* Endothelial NADPH oxidase-2 promotes interstitial cardiac fibrosis and diastolic dysfunction through proinflammatory effects and endothelial-mesenchymal transition. *J. Am. Coll. Cardiol.* **63,** 2734–2741 (2014).
21. Charytan, D. M. *et al.* Increased concentration of circulating angiogenesis and nitric oxide inhibitors induces endothelial to mesenchymal transition and myocardial fibrosis in patients with chronic kidney disease. *Int. J. Cardiol.* **176,** 99–109 (2014).
22. Ma, K. L. *et al.* Inflammatory stress exacerbates the progression of cardiac fibrosis in high-fat-fed apolipoprotein E knockout mice via endothelial-mesenchymal transition. *Int J Med Sci*. **10,** 420–426 (2013).
23. Widyantoro, B. *et al.* Endothelial cell-derived endothelin-1 promotes cardiac fibrosis in diabetic hearts through stimulation of endothelial-to-mesenchymal transition. *Circulation*. **121,** 2407–2418 (2010).
24. Mathews, V. V. *et al.* Myocardial toxicity of acute promyelocytic leukaemia drug-arsenic trioxide. *Eur Rev Med Pharmacol Sci*. **17** Suppl 1, 34–38 (2013).
25. Patel, S. P. *et al.* Cardiotoxicity in African-American patients treated with arsenic trioxide for acute promyelocytic leukemia. *Leuk Res*. **30,** 362–363 (2006).
26. Yoshimatsu, Y. & Watabe, T. Roles of TGF-beta signals in endothelial-mesenchymal transition during cardiac fibrosis. *Int J Inflam.* **2011,** 724080 (2011).
27. Gasperini, P. *et al.* Kaposi sarcoma herpesvirus promotes endothelial-to-mesenchymal transition through Notch-dependent signaling. *Cancer Res*. **72,** 1157–1169 (2012).
28. Curci, C. *et al.* Endothelial-to-mesenchymal transition and renal fibrosis in ischaemia/reperfusion injury are mediated by complement anaphylatoxins and Akt pathway. *Nephrol Dial Transplant*. **29,** 799–808 (2014).
29. Yan, F. *et al.* Glucagon-Like Peptide 1 Protects against Hyperglycemic-Induced Endothelial-to-Mesenchymal Transition and Improves Myocardial Dysfunction by Suppressing Poly(ADP-Ribose) Polymerase 1 Activity. *Mol. Med.* **21,** 15–25 (2015).
30. Zhou, S. L. *et al.* CXCR2/CXCL5 axis contributes to epithelial-mesenchymal transition of HCC cells through activating PI3K/Akt/GSK-3beta/Snail signaling. *Cancer Lett*. **358,** 124–135 (2015).
31. Liu, L. *et al.* Maelstrom promotes hepatocellular carcinoma metastasis by inducing epithelial-mesenchymal transition by way of Akt/GSK-3beta/Snail signaling. *Hepatology*. **59,** 531–543 (2014).
32. Morita, N., Mandel, W. J., Kobayashi, Y. & Karagueuzian, H. S. Cardiac fibrosis as a determinant of ventricular tachyarrhythmias. *J Arrhythm*. **30,** 389–394 (2014).
33. Tamaki, S. *et al.* Interleukin-16 promotes cardiac fibrosis and myocardial stiffening in heart failure with preserved ejection fraction. *PLoS One*. **8,** e68893 (2013).
34. Shen, Z. X. *et al.* Use of arsenic trioxide (As2O3) in the treatment of acute promyelocytic leukemia (APL): II. Clinical efficacy and pharmacokinetics in relapsed patients. *Blood*. **89,** 3354–3360 (1997).
35. Rock, N. *et al.* Treatment of an acute promyelocytic leukemia relapse using arsenic trioxide and all-trans-retinoic in a 6-year-old child. *Pediatr Hematol Oncol*. **31,** 143–148 (2014).
36. Sun, H. L. *et al.* Choline-modulated arsenic trioxide-induced prolongation of cardiac repolarization in Guinea pig. *Basic Clin Pharmacol Toxicol*. **98,** 381–388 (2006).
37. Shen, N. *et al.* Shensong Yangxin Capsule prevents diabetic myocardial fibrosis by inhibiting TGF-beta1/Smad signaling. *J. Ethnopharmacol.* **157,** 161–170 (2014).
38. Qin, W. *et al.* Genistein alleviates pressure overload-induced cardiac dysfunction and interstitial fibrosis in mice. *Br J Pharmacol*. **172,** 5559–5572 (2015).
39. Tang, R. *et al.* Angiotensin II mediates the high-glucose-induced endothelial-to-mesenchymal transition in human aortic endothelial cells. *Cardiovasc Diabetol*. **9,** 31 (2010).
40. Montorfano, I. *et al.* Oxidative stress mediates the conversion of endothelial cells into myofibroblasts via a TGF-beta1 and TGF-beta2-dependent pathway. *Lab. Invest.* **94,** 1068–1082 (2014).
41. Zeisberg, E. M., Potenta, S. E., Sugimoto, H., Zeisberg, M. & Kalluri, R. Fibroblasts in kidney fibrosis emerge via endothelial-to-mesenchymal transition. *J. Am. Soc. Nephrol.* **19,** 2282–2287 (2008).
42. Zeisberg, E. M., Potenta, S., Xie, L., Zeisberg, M. & Kalluri, R. Discovery of endothelial to mesenchymal transition as a source for carcinoma-associated fibroblasts. *Cancer Res*. **67,** 10123–10128 (2007).
43. Maseki, S. *et al.* Acquisition of EMT phenotype in the gefitinib-resistant cells of a head and neck squamous cell carcinoma cell line through Akt/GSK-3beta/snail signalling pathway. *Br J Cancer*. **106,** 1196–1204 (2012).
44. Li, Z. & Jimenez, S. A. Protein kinase Cdelta and c-Abl kinase are required for transforming growth factor beta induction of endothelial-mesenchymal transition *in vitro*. *Arthritis. Rheum.* **63,** 2473–2483 (2011).
45. Medici, D., Potenta, S. & Kalluri, R. Transforming growth factor-beta2 promotes Snail-mediated endothelial-mesenchymal transition through convergence of Smad-dependent and Smad-independent signalling. *Biochem. J.* **437,** 515–520 (2011).
46. You, B. R. & Park, W. H. Arsenic trioxide induces human pulmonary fibroblast cell death via increasing ROS levels and GSH depletion. *Oncol Rep*. **28,** 749–757 (2012).
47. Shan, H. *et al.* Upregulation of microRNA-1 and microRNA-133 contributes to arsenic-induced cardiac electrical remodeling. *Int. J. Cardiol.* **167,** 2798–2805 (2013).
48. Hu, Y. *et al.* Bisphenol A, an environmental estrogen-like toxic chemical, induces cardiac fibrosis by activating the ERK1/2 pathway. *Toxicol. Lett.* **250–251,** 1–9 (2016).
49. Zhang, Y. *et al.* Berberine hydrochloride prevents postsurgery intestinal adhesion and inflammation in rats. *J. Pharmacol. Exp. Ther.* **349,** 417–426 (2014).
50. Li, X. *et al.* MicroRNA-30d regulates cardiomyocyte pyroptosis by directly targeting foxo3a in diabetic cardiomyopathy. *Cell Death and Disease*. **5,** e1479 (2014).
51. Zhang, T. *et al.* Downregulation of miR-522 suppresses proliferation and metastasis of non-small cell lung cancer cells by directly targeting DENN/MADD domain containing 2D. *Sci Rep*. **6,** 19346 (2016).
52. Xu, C. *et al.* beta-Blocker carvedilol protects cardiomyocytes against oxidative stress-induced apoptosis by up-regulating miR-133 expression. *J Mol Cell Cardiol*. **75,** 111–121 (2014).
53. Zhang, Y. *et al.* MicroRNA-26a prevents endothelial cell apoptosis by directly targeting TRPC6 in the setting of atherosclerosis. *Sci. Rep*. **5,** 9401 (2015).

Acknowledgements

This work was supported by the Funds for Creative Research Groups (81421063) and the National Natural Science Foundation of China (81570399, 81270042, 30901208) and the Program for New Century Excellent Talents In Heilongjiang Provincial University (1254-NCET-012).

Author Contributions

B.Y. and Yong Z. designed the study. X.W., Y.L., H.Z., Z.L., Ying Z., L.Z., J.J., X.C., X.L., V.N. and P.K. carried out data acquisition and analysis. Yong Z., X.W. and Y.L. wrote the paper. C.X., B.Y. and P.V.G. supervised the study. All authors reviewed the manuscript.

Additional Information

Supplementary information accompanies this paper at http://www.nature.com/srep

Competing financial interests: The authors declare no competing financial interests.

How to cite this article: Zhang, Y. *et al.* Endothelial to mesenchymal transition contributes to arsenic-trioxide-induced cardiac fibrosis. *Sci. Rep.* **6**, 33787; doi: 10.1038/srep33787 (2016).